

Solution-State, Solid-State, and Calculated Structures of an α -Lithiated Monophosphazene[†]

Fernando López-Ortiz,^{*,‡} Elvira Peláez-Arango,[‡] Baudilio Tejerina,[§] Enrique Pérez-Carreño,[§] and Santiago García-Granda[§]

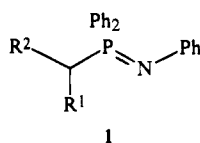
Contribution from the Instituto Universitario de Química Organometálica Enrique Moles, Unidad Asociada al CSIC, Universidad de Oviedo, 33071 Oviedo, Spain, and Departamento de Química Física y Analítica, Universidad de Oviedo, 33071 Oviedo, Spain

Received April 3, 1995[®]

Abstract: The structure of lithiated *P*-diphenyl(methyl)(*N*-phenyl)phosphazene (Li^+1a^-) has been determined. The crystal structure consists of monomeric units containing a four-membered ring with the lithium bonded to the nitrogen and methylene carbon atoms of the phosphazene. The coordination sphere of the metal is completed by two molecules of THF. The carbon bonded to lithium has a pyramidal configuration. Short intermolecular Li-phenyl-P distances (average 3.10 Å) have been measured in the crystal packing. In THF at $-111\text{ }^\circ\text{C}$, a 93:7 mixture of two compounds was found. The structure of the major component was determined by multinuclear ^1H , ^6Li , ^{13}C , ^{15}N , and ^{31}P NMR spectroscopy of isotopically labeled $^6\text{Li}^+1\text{a}^-$. From the $^2J_{\text{PLi}}$ -coupling constant measured and the NOEs observed in 2D HOESY spectra, it was concluded that the major component retained a structure similar to that found in the solid state. ^{15}N Characterization was carried out through ^{31}P , ^{15}N triple resonance experiments. MNDO calculations reproduced well the main structural features of Li^+1a^- . Two local minima interconnected by two transition states were located through MNDO calculations. The preference for the formation of the C-P-N-Li four-membered ring was considered to be of electrostatic nature. No P-Li bonding interaction was predicted, and the calculated dissociation energy for the C-Li was $30.8\text{ kcal}\cdot\text{mol}^{-1}$.

Introduction

Heteroatom-stabilized anions are among the most useful synthetic intermediates for carbon-carbon bond formation.¹ Particularly, those derived from phosphorus compounds have played a dominant role in the construction of C-C single and double bonds. Phosphine oxides² or phosphonates,³ phosphon-diamides,⁴ and their thio derivatives⁵ have been mainly used for that purpose. In recent years we have shown that anions of *N*-aryl(alkyl)-*p*-diarylmonophosphazenes **1** can also be added



- 1a:** R¹ = R² = H
1b: R¹ = H; R² = CH₃
1c: R¹ = H; R² = C₂H₅
1d: R¹ = H; R² = CH₂CH=CH₂
1e: R¹ = R² = CH₃
1f: R¹ = CH₃; R² = C₂H₅
1g: R¹ = C₂H₅; R² = C₆H₅

to different electrophiles with excellent regio- and stereochemical control of the reaction course.⁶ Furthermore, stepwise

processes combining the reactivity of the P=N linkage and the α -position of phosphazenes allowed several phosphorus-containing heterocycles of previously unknown structure to be obtained.⁷ In order to understand the selectivity observed and to explore the applications of phosphazenylium anions in asymmetric synthesis in a rational way, an accurate model of their structure is required.

Excluding ylides, structural studies on phosphorus-stabilized anions are scarce. The first attempts to elucidate the solution

(3) (a) Wadsworth, W. S., Jr. *Org. React.* **1977**, *25*, 73. (b) Kirilov, M.; Petrov, G. *Monatsh. Chem.* **1968**, *99*, 148; (c) *Tetrahedron Lett.* **1970**, 129; (d) **1972**, 4487; (e) *Phosphorus Sulfur* **1980**, *9*, 87. (f) Amer, A.; Zimmer, H. In *Handbook of Organophosphorus Chemistry*; Engel, R., Ed.; Marcel Dekker: New York, 1992; Chapter 6. (g) Mastalerz, P. In ref 3f, Chapter 7. (h) Mikolajczyk, M.; Mikina, M. *J. Org. Chem.* **1994**, *59*, 6760.

(4) (a) Denmark, S. E.; Dorow, R. L. *J. Org. Chem.* **1990**, *55*, 5926. (b) Denmark, S. E.; Stadler, H.; Dorow, R. L.; Kim, J. H. *J. Org. Chem.* **1991**, *56*, 5063. (c) Denmark, S. E.; Chatani, N.; Pansare, S. V. *Tetrahedron* **1992**, *48*, 2191. (d) Denmark, S. E.; Chen, C.-T. *J. Am. Chem. Soc.* **1992**, *114*, 10674. (e) Denmark, S. E.; Amburgey, J. *J. Am. Chem. Soc.* **1993**, *115*, 10386. (f) Denmark, S. E.; Chen, C. T. *J. Org. Chem.* **1994**, *59*, 2922.

(5) For thiophosphonates, see: (a) Corey, E. J.; Kwiatkowski, G. T. *J. Am. Chem. Soc.* **1966**, *88*, 5654. For thiophosphinamides, see: (b) Johnson, C. R.; Elliott, R. C. *J. Am. Chem. Soc.* **1982**, *104*, 7041. (c) Denmark, S. E.; Swiss, K. A. *J. Am. Chem. Soc.* **1993**, *115*, 12195. For bis(phosphine sulfides), see: (d) Goli, M. B.; Grim, S. O. *Tetrahedron Lett.* **1991**, 3631.

(6) (a) For an early work on the metalation of *N*-arylmonophosphazenes, see: (a) Stuckwisch, C. G. *J. Org. Chem.* **1976**, *41*, 1173. (b) Barluenga, J.; López, F.; Palacios, F. *J. Chem. Res. (S)* **1985**, 211. (c) Barluenga, J.; López, F.; Palacios, F.; Cano, F. H.; Foces-Foces, M. *J. Chem. Soc., Perkin Trans. 1* **1988**, 2329. (d) Barluenga, J.; López, F.; Palacios, F. *Synthesis* **1988**, 562; (e) **1989**, 289. For metalated *N*-(trimethylsilyl) derivatives, see: (f) Schmidbauer H.; Jonas, G. *Chem. Ber.* **1967**, *100*, 1120. (g) Wettermark, U. G.; Wisian-Neilson, P.; Scheide, G. M.; Neilson, R. H. *Organometallics* **1987**, *6*, 959 and references therein. Metalations of cyclotriphosphazenes^{6h,i} and polyphosphazenes^{6j} have also been described: (h) Calhoun, H. P.; Lindstrom, R. H.; Oakley, R. T.; Paddock, N. L.; Todd, S. M. *J. Chem. Soc., Chem. Commun.* **1975**, 343. (i) Galliciano, K. D.; Oakley, R. T.; Paddock, N. L.; Sharma, R. D. *Can. J. Chem.* **1981**, *59*, 2654. (j) Neilson, R. H.; Wisian-Neilson, P. *Chem. Rev.* **1988**, *88*, 541.

(7) (a) Barluenga, J.; López, F.; Palacios, F. *J. Chem. Soc., Chem. Commun.* **1985**, 1681; (b) **1986**, 1574; (c) *Tetrahedron Lett.* **1987**, *28*, 2875; (d) *J. Organomet. Chem.* **1990**, *382*, 61.

[†] Dedicated to Prof. H. Günther on the occasion of his 60th birthday.
[‡] Instituto Universitario de Química Organometálica Enrique Moles.
[§] Departamento de Química Física y Analítica.

[®] Abstract published in *Advance ACS Abstracts*, August 15, 1995.

(1) (a) Evans, D. A.; Andrews, G. C. *Acc. Chem. Res.* **1974**, *7*, 147. (b) Magnus, P. D. *Tetrahedron* **1977**, *33*, 2019. (c) Beak, P.; Reitz, D. B. *Chem. Rev.* **1978**, *78*, 275. (d) Krief, A. *Tetrahedron* **1980**, *36*, 2531. (e) Solladie, G. *Synthesis* **1981**, 185. (f) Werstiuk, N. H. *Tetrahedron* **1983**, *39*, 205. (g) Hoppe, D. *Angew. Chem., Int. Ed. Engl.* **1984**, *23*, 932. (h) Oae, S.; Uchida, Y. In *The Chemistry of Sulfones and Sulfoxides*; Sterling, C. J. M., Patai, S., Rappoport, Z., Eds.; Wiley-Interscience: New York, 1988; Chapter 12.

(2) (a) *Organophosphorus Reagents in Organic Synthesis*; Cadogan, J. I. G., Ed.; Academic Press: New York, 1980. (b) Maryanoff, B. E.; Reitz, A. B. *Chem. Rev.* **1989**, *89*, 863. (c) Edmundson, R. S. In *The Chemistry of Organophosphorus Compounds*; Hartley, F. R., Ed.; Wiley-Interscience: New York, 1992; Vol. 2, Chapter 7.

structure of phosphorus-containing anionic species were by the groups of Kirilov⁸ and Seyden-Penne.⁹ These works were based on the analysis of IR and NMR spectra of Horner^{10a} or Wadsworth–Emmons reagents,^{10b} i.e., α -lithiated phosphine oxides and phosphonic acid esters, respectively. More recently, Denmark *et al.* have contributed significantly to this area through detailed solid-state and solution studies on lithiated phosphonamides.¹¹

A major difficulty concerning the structural elucidation of organolithium compounds in solution is their association behavior, which may vary depending on the reaction conditions¹² and may even differ from that found in the solid state.¹³ The classical methods of determination of the aggregation state in solution are based on colligative properties.¹⁴ However, NMR spectroscopy has additional advantages due to its simplicity and higher information content.¹⁵ The method relies on the existence of a scalar coupling between lithium and a directly bonded nucleus. For this coupling to be observed two criteria have to

be met: (i) slow interaggregate exchange in the NMR time scale and (ii) slow relaxation of the lithium nucleus. The first condition can generally be fulfilled by working at very low temperatures. The second suggests a preference for the ⁶Li over the ⁷Li isotope because of its low quadrupolar moment,^{15b} although coupling constants to ⁶Li are lower than those to ⁷Li by a factor of 2.64 ($\gamma^7\text{Li}/\gamma^6\text{Li}$).

A common feature of organolithium phosphorus(V) compounds containing P=X (X = N, O, S) groups is the lack of a carbon–lithium bond, a situation similar to that found in monometalated sulfoxides¹⁶ and sulfones.^{13e,16} In this paper we report the first single-crystal X-ray and solution structure of a lithium monophosphazene derivative showing the existence of a nitrogen– and a carbon–lithium bond. These results are compared with the theoretical structure obtained by MNDO calculations. The X-ray analysis has been carried out on crystals formed in a THF solution. The solution structure has been derived from a multinuclear NMR study (¹H, ⁶Li, ¹³C, ¹⁵N, and ³¹P), including several combinations of triple resonance experiments. The effect of metalation of **1a** on several NMR parameters is discussed in terms of changes in geometry and charge distribution versus the parent compound, and the results are in good agreement with those expected from the computed structure. The stability of the ring formed between the bidentate phosphazene ligand and the lithium was analyzed according to the MNDO method.

Experimental Section

General. All manipulations were carried out using inert atmosphere techniques or in a MBraun MB 150-GI drybox. Isotopically labeled [⁶Li]-*n*-butyllithium–hexane solutions were prepared according to the Gilman method.¹⁷ ⁶Li 96% (Aldrich) was used, and the concentration was determined by double titration with 0.1 N HCl. Solvents (THF and THF-*d*₈) were freshly distilled from potassium benzophenone ketyl and degassed three times prior to use. NMR samples were flame sealed and stored at –30 °C.

X-ray Crystallography. Suitable single crystals were selected, mounted at room temperature, and immediately placed in the low-temperature nitrogen stream at 200 K. X-ray data were collected with an Enraf-Nonius CAD4 diffractometer (Mo K α radiation, graphite monochromator, $\lambda = 0.71073$ Å) equipped with a low-temperature device. The structure was solved by Patterson interpretation and phase expansion (DIRDIF),¹⁸ and the refinement was performed by full-matrix least-squares procedures (SHELX76).¹⁹ Hydrogen atoms were refined isotropically riding on their parent atom with a common thermal parameter. All calculations were made at the University of Oviedo on the Scientific Computer Center and X-Ray Group Vax computers. Crystal data: C₂₇H₃₃LiNO₂P, MW = 441.48, monoclinic, space group C2/c, $a = 31.76(6)$ Å, $b = 9.69(1)$ Å, $c = 17.8(1)$ Å, $\beta = 115.8(4)^\circ$, $V = 4930(47)$ Å³, $Z = 8$, $D_x = 1.19$ g/cm³, $\mu = 1.29$ cm⁻¹, $F(000) = 1888$, $T = 200(2)$ K, $R = 0.048$, and $R_w = 0.044$ for 1438 observed reflections and 281 variables.

Preparation of the Lithium *N*-Phenylmethylenediphenylphosphazene Complex. Methylidiphenylphosphazene (5 g, 17.2 mmol) in 10 mL of dry THF were added dropwise to an *n*-butyllithium–hexane solution (7.2 mL, 18.1 mmol) at –30 °C. The yellow solution was

(8) (a) Kirilov, M.; Petrov, G. *Chem. Ber.* **1971**, *104*, 3073; (b) *Monatsh. Chem.* **1972**, *103*, 1651.

(9) (a) Bottin-Strzalko, T.; Seyden-Penne, J.; Simonnin, M.-P. *J. Chem. Soc., Chem. Commun.* **1976**, 905; (b) *J. Org. Chem.* **1978**, *43*, 4346. (c) Bottin-Strzalko, T.; Corset, J.; Froment, F.; Pouet, M.-J.; Seyden-Penne, J.; Simonnin, M.-P. *J. Org. Chem.* **1980**, *45*, 1270. (d) Seyden-Penne, J. *Bull. Soc. Chim. Fr.* **1987**, 238. (e) Bottin-Strzalko, T.; Seyden-Penne, J.; Froment, F.; Corset, J.; Simonnin, M.-P. *J. Chem. Soc., Perkin Trans. 2* **1987**, 783; (f) *Can. J. Chem.* **1988**, *66*, 391. See also: (g) Colquhoun, J.; Christina, H.; McFarlane, E.; McFarlane, W. *J. Chem. Soc., Chem. Commun.* **1982**, 220. (h) Teulade, M.-P.; Savignac, P.; About-Jaudet, E.; Collignon, N. *Phosphorus Sulfur* **1988**, *40*, 105. (i) Yuan, C.; Yao, J.; Li, S.; Mo, Y.; Zhong, X. *Phosphorus Sulfur* **1989**, *46*, 25. (j) Patios, C.; Ricard, L.; Savignac, P. *J. Chem. Soc., Perkin Trans. 1* **1990**, 1577. (k) Yao, C. Y. J.; Li, S. *Phosphorus Sulfur* **1990**, *53*, 21.

(10) (a) Horner, L.; Hoffmann, H.; Wippel, H. G. *Chem. Ber.* **1958**, *91*, 61. (b) Wadsworth, W. S.; Emmons, W. D. *J. Am. Chem. Soc.* **1961**, *83*, 1733. See also ref 2 and 3.

(11) (a) Denmark, S. E.; Dorow, R. L. *J. Am. Chem. Soc.* **1990**, *112*, 864. (b) Denmark, S. E.; Miller, P. C.; Wilson, S. R. *J. Am. Chem. Soc.* **1991**, *113*, 1468. (c) Denmark, S. E.; Swiss, K. A.; Wilson, S. R. *J. Am. Chem. Soc.* **1993**, *115*, 3826. (d) Denmark, S. E.; Swiss, K. A. *J. Am. Chem. Soc.* **1993**, *115*, 12195. X-ray structures of phosphorus-stabilized anions of magnesium and copper salts of keto phosphonates^{11e,f} and lithiophosphinomethanides^{11g-k} have been reported. For leading references, see, for example: (e) Weiss, E.; Kopf, J.; Gardein, T.; Cornellin, S.; Schumann, U.; Kirilov, M.; Petrov, G. *Chem. Ber.* **1985**, *118*, 3529. (f) Macicek, J.; Angelova, O.; Petrov, G.; Kirilov, M. *Acta Crystallogr., Sect. C* **1988**, *44*, 626. (g) Byrne, L. T.; Engelhardt, L. M.; Jacobsen, G. E.; Leung, W.-P.; Papasergio, R. I.; Raston, C. L.; Skelton, B. W.; Twiss, P.; White, A. H. *J. Chem. Soc., Dalton Trans.* **1989**, 105. (h) Fraenkel, G.; Winchester, W. R.; Willard, P. G. *Organometallics* **1989**, *8*, 2308. (i) Karsch, H. H.; Richter, R.; Paul, M.; Riede, J. *J. Organomet. Chem.* **1994**, *474*, C1 and references therein. (j) Winkler, M.; Lutz, M.; Müller, G. *Angew. Chem., Int. Ed. Engl.* **1994**, *33*, 2279. (k) Pape, A.; Lutz, M.; Müller, G. *Angew. Chem., Int. Ed. Engl.* **1994**, *33*, 2281.

(12) (a) Schlosser, M. In *Organometallics in Synthesis, a Manual*; Schlosser, M., Ed.; John Wiley: New York, 1994; Chapter 1. (b) Wardell, J. L. In *Comprehensive Organometallic Chemistry*; Wilkinson, G., Stone, F. G. A., Abel, E. W., Eds.; Pergamon Press: Oxford, 1982; Vol. 1, Chapter 2.

(13) Reviews: (a) Setzer, W. N.; Schleyer, P. v. R. *Adv. Organomet. Chem.* **1985**, *24*, 353. (b) Schade, C.; Schleyer, P. v. R. *Adv. Organomet. Chem.* **1987**, *27*, 169. (c) Williard, P. G. In *Comprehensive Organic Synthesis*; Trost, B. M., Fleming, Y., Schreiber, S. L., Eds.; Pergamon Press: Oxford, 1991; Vol. 1, Chapter 1. (d) Seebach, D. *Angew. Chem., Int. Ed. Engl.* **1988**, *27*, 1624. (e) Boche, G. *Angew. Chem., Int. Ed. Engl.* **1989**, *28*, 277. (f) Markies, P. R.; Akkerman, O. S.; Bickelhaupt, F.; Smeets, W. J. J.; Spek, A. L. *Adv. Organomet. Chem.* **1991**, *32*, 147. (g) Gregory, K.; Schleyer, P. v. R.; Snaith, R. *Adv. Inorg. Chem.* **1991**, *37*, 47. (h) Mulvey, R. *Chem. Soc. Rev.* **1991**, *20*, 167. (i) Hanusa, T. P. *Chem. Rev.* **1993**, *93*, 1023. (j) Weiss, E. *Angew. Chem., Int. Ed. Engl.* **1993**, *32*, 1501.

(14) (a) Bauer, W.; Seebach, D. *Helv. Chim. Acta* **1988**, *67*, 1972 and references therein. (b) Davidson, M. G.; Snaith, R.; Stalke, D.; Wright, D. S. *J. Org. Chem.* **1993**, *58*, 2810.

(15) Reviews: (a) Günther, H.; Moskau, D.; Bast, P.; Schmalz, D. *Angew. Chem., Int. Ed. Engl.* **1987**, *26*, 1212. (b) Akit, J. W. In *Multinuclear NMR*; Mason, J., Ed.; Plenum Press: New York, 1987; Chapter 7, p 189. (c) Thomas, R. D. In *Isotopes in the Physical and Biomedical Sciences*; Buncel, E., Jones, J. R., Eds.; Elsevier: Amsterdam, 1991; Vol. 2, Chapter 7. (d) Bauer, W.; Schleyer, P. v. R. *Adv. Carbanion Chem.* **1992**, *1*, 89.

(16) C–Li bonds have been observed in [(2,2-diphenyl-1-(phenylsulfonyl)cyclopropyl)lithium]; dimethoxetane^{16a} and dilithio[(trimethylphenyl)sulfonyl]methylsilane.^{16b} (a) Hollstein, W.; Harms, K.; Marsch, M.; Boche, G. *Angew. Chem., Int. Ed. Engl.* **1988**, *27*, 846. (b) Gais, H. J.; Vollhardt, H.; Günther, H.; Moskau, D.; Lindner, H. J.; Braun, S. *J. Am. Chem. Soc.* **1988**, *110*, 978.

(17) Gilman, H.; Beel, J. A.; Brannen, C. G.; Bullock, M. W.; Dunn, G. E.; Miller, L. S. *J. Am. Chem. Soc.* **1949**, *71*, 1499.

(18) Beurskens, P. T.; Admiraal, G.; Behm, H.; Beurskens, G.; Bosman, W. P.; García-Granda, S.; Gould, R. O.; Smykalla, C. The DIRDIF Program System. Technical Report of the Crystallography Laboratory, University of Nijmegen, The Netherlands, 1992.

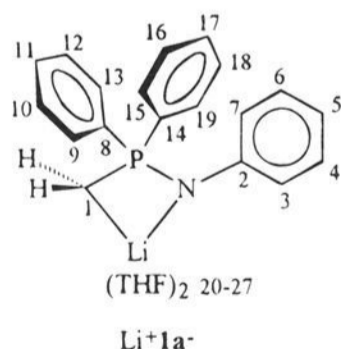
(19) Sheldrick, G. M. *SHELX, A Program for Crystal Structure Determination*; University Chemical Laboratory, Cambridge, England, 1976.

stirred for 2 h and then evaporated to dryness under reduced pressure. On addition of 5 mL of dry THF at $-30\text{ }^{\circ}\text{C}$, a precipitate formed. The yellow powder was filtered and redissolved in 10 mL of THF. On the solution standing at $-30\text{ }^{\circ}\text{C}$ for 1 week, colorless crystals were isolated and used for the X-ray and NMR studies.

NMR Spectroscopic Analysis. NMR spectra were run on a Bruker AMX400 spectrometer equipped with a third radio frequency channel. A 5 mm reverse triple probe head was used. The inner coil was doubly tuned for ^1H and ^{31}P , and the outer coil was tunable in the frequency range 18–160 MHz. The pulse widths for the 90° pulses and operating frequencies were 10.4 (^1H , 400 MHz), 17.1 (^{15}N , 40.5 MHz), 16.7 (^6Li , 58, MHz), 14.5 (^{13}C , 100.6 MHz), and $14.5\ \mu\text{s}$ (^{31}P , 161.98 MHz). The attenuation levels used were 5 dB for the proton channel and 3 dB for the heteronuclei. The spectral references used were tetramethylsilane for ^1H and ^{13}C , 85% H_3PO_4 for ^{31}P , neat nitromethane for ^{15}N , and 1 M LiBr in D_2O for ^6Li .

Selected spectral parameters were as follows. One-dimensional ^1H NMR: 32K data points; spectral width, 4000 Hz. ^{13}C NMR: 32K data point; spectral width, 18 000; exponential multiplication with a line broadening factor of 1 Hz. ^{31}P NMR: 32K data points; spectral width, 6000 Hz; exponential line broadening of 1 Hz. ^6Li NMR: 16K data points; spectral width, 600 Hz; exponential line broadening of 0.5 Hz. ^{15}N , ^{31}P INEPT: 32K data points; spectral width, 4000 Hz; exponential line broadening of 2 Hz. The experiment was conducted overnight because our probe head was designed for $^1\text{H}/^{31}\text{P}$ observation, and about 50% loss of sensitivity is estimated when a heteronucleus is directly observed through the broad band channel. ^6Li , ^1H 2D HOESY: spectral width, 200 Hz in F2 and 4000 Hz in F1; 48 increments recorded; final matrix after zero filling, 512×256 ; mixing time, 2.0 s; 40 scans/increment in F1; q sine multiplication of $\pi/2$ in both dimensions prior to transformation. ^{31}P , ^{13}C 2D HMQC: spectral width, 800 Hz in F2 and 1000 Hz in F1; 128 increments recorded; final matrix after zero filling, 1024×256 ; evolution delay of $^1J_{\text{PC}}$, 5.6 ms; 40 scans/increment in F1; q sine multiplication of $\pi/2$ in both dimensions prior to transformation. ^{31}P , ^{15}N 2D HMQC: spectral width, 800 Hz in F2 and 1000 Hz in F1; 96 increments recorded; final matrix after zero filling, 1024×256 ; evolution delay of $^1J_{\text{PN}}$, 18.7 ms; 200 scans/increment in F1; q sine multiplication of $\pi/2$ in both dimensions prior to transformation.

Computational Methods. Considering the large size of the molecules under issue, we have restricted our computational study to a semiempirical level of theory. MNDO calculations were carried out using the MOPAC²⁰ and GAMESS²¹ programs. The programs used depended upon the computational problem being treated. The stationary points located on the potential energy surface (PES) were characterized by harmonic vibrational frequencies analysis. The X-ray geometry of $\text{Li}^+\mathbf{1a}^-$ was used as a starting point for the calculations. The four-membered ring was forced to break by increasing the torsion angle C1–P1–N1–Li1 (see Figure 4).



Results

X-ray Crystallographic Analysis of $\text{Li}^+\mathbf{1a}^-$. The lithiated anion of $\mathbf{1a}$ (abbreviated as $\text{Li}^+\mathbf{1a}^-$) crystallizes from THF as a monomer with two molecules of solvent coordinated to the

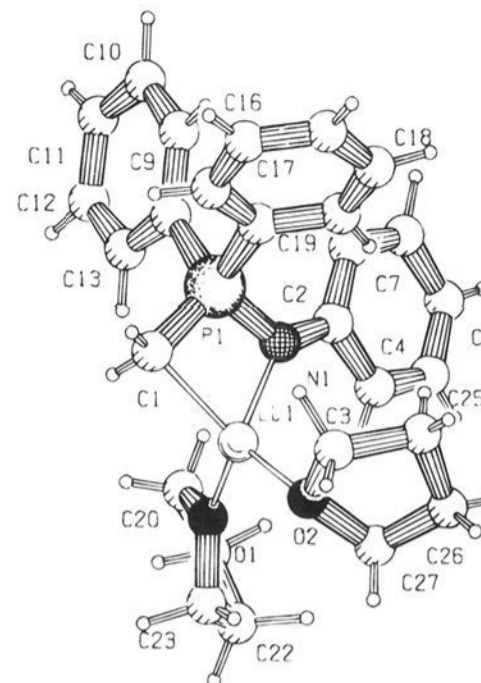


Figure 1. Molecular structure of compound $\text{Li}^+\mathbf{1a}^-$ determined by X-ray including the numbering scheme used. The H atoms are omitted for clarity.

lithium atom. The molecular structure and the adopted numbering scheme are shown in Figure 1. The unit cell and a detail of the crystal packing are included in the supporting information. Selected bond distances and angles are given in Table 1. The unit cell is formed by eight molecules arranged in pairs, where each lithium atom is close to one of the *P*-phenyl rings of a molecule belonging to a neighbor unit cell. The packing of the crystal consist of pairs of molecules affording a tridimensional figure resembling a helical structure. The shortest Li–H intermolecular distances were found for the meta protons of the corresponding aromatic rings (Li1–H10', average 3.1 Å).

The most important structural characteristic of $\text{Li}^+\mathbf{1a}^-$ is the four-membered ring formed by the P1–N1–Li1–C1 atoms, which implies that the lithium is bonded to both the nitrogen, 2.00(1) Å, and C1, 2.23(1) Å, atoms. The P–Li distance of 2.65(3) Å has a value appropriate for the existence of a bonding interaction,^{11k,22} but it must be borne in mind that the rigidity of the molecule would force these atoms to be close, anyway. The ring slightly deviates from planarity due to a displacement of $8.0(1)^{\circ}$ of the lithium atom above the plane defined by the C1–P1–N1 atoms. The lithium is solvated by two molecules of THF (average Li–O bond lengths 1.94 Å) and has a distorted tetrahedral coordination geometry, with a very small N1–Li1–C1 angle of $77.2(4)^{\circ}$, a constraint imposed by the chelating phosphazanyl anion. The other bond angles at lithium lie between $106.3(5)^{\circ}$ and $119.9(5)^{\circ}$.

The P atom shows a tetrahedral coordination, with bonding angles in the range of $105.0(2)$ – $115.5(3)^{\circ}$. It is interesting to point out the large angle of $105.6(3)^{\circ}$ formed by the C1–P1–N1 framework of the four-membered ring. The P–N bond distance of 1.614(4) Å is significantly shorter than a formal single bond (cf. values of 1.77²³ and 1.57 Å²⁴ for the formal P–N single and double bonds, respectively), which suggests a bond order larger than unity. Accordingly, the N1–C2 bond length of 1.381(5) Å is typical of planar N sp^2 bonded to a C sp^2 carbon.²⁵ The exocyclic bond angles involving the nitrogen are close to 120° , whereas a value of $93.4(4)^{\circ}$ is found for the

(20) (a) MOPAC: Stewart, J. J. P. *QCPE Bull.* **1990**, No. 445. (b) MNDO: Dewar, M. J. S.; Thiel, W. *J. Am. Chem. Soc.* **1977**, *99*, 4899, 4907.

(21) GAMESS: Schmidt, M. W.; Baldridge, K. K.; Boatz, J. A.; Elbert, S. T.; Gordon, M. S.; Jensen, J. H.; Koseki, S.; Matsunaga, N.; Nguyen, K. A.; Su, S. J.; Windus, T. L.; Duouis, M.; Montgomery, J. A. *J. Comput. Chem.* **1993**, *14*, 1347.

(22) Compare: (a) P–Li [(TMEDA)LiClAlMe₂C(SiMe₃)₂PMe₂] = 2.67 Å (Karsh, H. H.; Zellner, K.; Müller, G. *Organometallics* **1991**, *10*, 2884). (b) P–Li(mean) [[LiP(SiMe₃)₂]₆] = 2.51 Å (Hey-Hawkins, E.; Sattler, E. *J. Chem. Soc., Chem. Commun.* **1992**, 775).

(23) Allcock, H. R. *Chem. Rev.* **1972**, *72*, 315.

(24) Hewlins, M. J. E. *J. Chem. Soc. (B)* **1971**, 942.

(25) Allen, F. H.; Kennard, O.; Watson, D. G.; Brammer, L.; Orpen, A. G.; Taylor, R. *J. Chem. Soc., Perkin Trans. 2* **1987**, S1.

Table 1. Selected Bond Lengths (Å), Bond Angles (deg), and Torsion Angles (deg) of $\text{Li}^+\mathbf{1a}^-$

bond lengths		bond angles		torsion angles	
P1-N1 = 1.614(4)		C1-P1-N1 = 105.6(3)		C1-P1-N1-Li1 = 8.(1)	
P1-C1 = 1.707(7)		Li1-N1-P1 = 93.4(4)		C1-P1-N1-C2 = -162.(2)	
P1-C8 = 1.817(3)		C1-Li-N1 = 77.2(4)		C1-P1-C8-C13 = 55.(2)	
P1-C14 = 1.813(3)		Li1-C1-P1 = 83.0(4)		C1-P1-C14-C19 = -69.(2)	
C1-Li1 = 2.23(1)		C2-N1-P1 = 129.5(4)		P1-N1-C2-C3 = 172.(2)	
N1-Li1 = 2.00(1)		C8-P1-C1 = 115.5(3)		P1-N1-Li1-O1 = 113.(1)	
N1-C2 = 1.381(5)		C8-P1-C14 = 105.0(2)		Li1-N1-C2-C3 = 6.(3)	
Li1-O1 = 1.94(1)		O1-Li1-O2 = 106.3(5)		C8-P1-N1-C2 = -37.(2)	
Li1-O2 = 1.95(1)		H1-C1-H2 = 114.0(6)		C8-P1-N1-Li1 = 133.(1)	
		H1-C1-P1 = 115.0(4)		C8-P1-C14-C19 = 106.(2)	

Table 2. Selected NMR Data for ${}^6\text{Li}^+\mathbf{1a}^-$ Recorded at $-111\text{ }^\circ\text{C}$ in $\text{THF-}d_8^a$

$\delta\text{ }^1\text{H}$ ($\Delta\delta$) (ppm)		$\delta\text{ }^{13}\text{C}$ ($\Delta\delta$) (ppm)		$\delta\text{ }^{31}\text{P}$	$\delta\text{ }^{15}\text{N}$	nJ (ΔJ) (Hz)				
H1	H3	C1	C8/C14	($\Delta\delta$) (ppm)	($\Delta\delta$) (ppm)	${}^1J_{\text{PC1}}$	${}^1J_{\text{PC8/C14}}$	${}^1J_{\text{PN}}$	${}^2J_{\text{PH}}$	
-0.08 (-2.44)	6.45 (0.25)	7.39 (-6.23)	140.36 (5.83)	23.73 (21.69)	-274.56 (24.6)	90.1 (27.7)	69.5 (-29.0)	26.8 (-9.8)	0.8 (-12.1)	

^a $\Delta\delta$ or ΔJ is referenced to the difference between the metalated and neutral **1a**. Positive $\Delta\delta$ numbers are downfield shifts.

inner P1-N1-Li1 angle. The P1-C1 bond distance of 1.707(7) Å is closer to a formal single bond (1.80 Å)²⁶ than to a formal double bond (1.57 Å). The sum of bond angles of C1 is only 343° on average, thus indicating a pyramidal configuration for C1. However, a P1-C1-Li1 angle of 83.0(4)° is found as consequence of the four-membered ring to which C1 belongs.

The aromatic rings at phosphorus are arranged nearly perpendicular to each other (the angle between the planes formed by the rings is 101.7(6)°), whereas the phenyl ring bonded to nitrogen lies slightly rotated from the plane defined by C1-P1-N1 (torsion angle P1-N1-C2-C3 of 172.0(2)°) in the same sense as the lithium atom does. As a result, H3 approaches Li1 at a distance as short as 2.89(1)Å.

Solution Structure of $\text{Li}^+\mathbf{1a}^-$ in THF. Crystals of ${}^6\text{Li}^+\mathbf{1a}^-$ were dissolved in $\text{THF-}d_8$, and the NMR spectra were recorded at different temperatures. Samples with lithium in natural abundance afforded very broad signals, which prevented a detailed analysis. The following discussion refers to 0.2 M samples 95% enriched in the ${}^6\text{Li}$ isotope and measured at $-111\text{ }^\circ\text{C}$, unless otherwise stated.

${}^1\text{H}$ and ${}^{13}\text{C}$ NMR Spectra. Metalation of **1a** is accompanied by marked changes in chemical shifts and coupling constants in the ${}^1\text{H}$ and ${}^{13}\text{C}$ NMR spectra (Table 2). All the proton and protonated carbon signals shift to higher field with regard to the neutral compound. The largest shielding affects the methylene group ($\Delta\delta_{\text{H}} = -2.44$ ppm, $\Delta\delta_{\text{C}} = -6.23$ ppm; $\Delta\delta = \delta(\text{anion}) - \delta(\text{neutral})$), but it is also worth mentioning the upfield shifts of 0.25 and 0.36 ppm of the ortho protons of the phenyl rings bonded to nitrogen and phosphorus, respectively. On the contrary, the quaternary carbons of ${}^6\text{Li}^+\mathbf{1a}^-$ are deshielded compared to **1a**, and again the largest effect occurs at C8/C14. Interestingly, at $-111\text{ }^\circ\text{C}$, a small hump appears in the ${}^1\text{H}$ NMR spectrum at the base of the signals for H9/H13/H15/H19 as well as H1/H2, thus indicating the existence of an equilibrium at least between two species, which are present in very different concentrations. Coalescence takes place at $-93\text{ }^\circ\text{C}$.

The ${}^1\text{H}$ NMR spectrum shows a doublet for H1/H2 of ${}^2J_{\text{PH}} = 0.8$ Hz at room temperature, which is not resolved at lower temperatures due to the line broadening. Large changes in coupling constants are also found in the ${}^{13}\text{C}$ NMR spectrum, especially for ${}^1J_{\text{PC}}$ of C1 ($\Delta J = 27.7$ Hz; $\Delta J = J(\text{anion}) - J(\text{neutral})$) and C8/C14 ($\Delta J = -29.0$ Hz). The effect of

metalation extends to C2, which is observed as a clear doublet of ${}^2J_{\text{PC}} = 5.1$ Hz. However, ${}^1J_{\text{CH}} = 132.9$ Hz for C1 increases only moderately ($\Delta J = 6.5$ Hz), indicating a very small increase in s character, i.e., C1 remains sp^3 hybridized in metalated **1a**. On the other hand, C1 shows a half-width of 20 Hz, and no ${}^6\text{Li}$, ${}^{13}\text{C}$ -coupling is resolved. Among other causes, broad signals may be related to intermolecular aggregation, which in turn are favored by high concentrations. Therefore, a dilute sample of ${}^6\text{Li}^+\mathbf{1a}^-$ (0.1 M) was prepared and the ${}^{13}\text{C}$ NMR spectrum measured. At this concentration, the measured line width of 16 Hz for C1 is still too large to resolve any ${}^{13}\text{C}$, ${}^6\text{Li}$ -coupling, even with resolution enhancement processing of the FID.

${}^{31}\text{P}$ NMR Spectra. The ${}^{31}\text{P}$ NMR spectrum of ${}^6\text{Li}^+\mathbf{1a}^-$ shows two resonances at 23.73 and 30.76 ppm in an approximate ratio of 93:7 and with half-widths of 13 and 31 Hz, respectively (Figure 2a). Line narrowing was observed when a more diluted sample was used (0.1 M, 11 Hz for the major and 25 Hz for the minor components), but no ${}^{31}\text{P}$, ${}^6\text{Li}$ -coupling could be detected in any case. These two signals merged at $-72\text{ }^\circ\text{C}$ into a singlet at 23.78 ppm. Some other very small signals that could be distinguished in the spectrum were assigned to impurities because their temperature line widening and coalescence were not related to major signals. They amount to <2% of the mixture on freshly prepared samples, and their concentration slowly increases with time even though the samples are sealed and maintained at temperatures below $-30\text{ }^\circ\text{C}$.

${}^6\text{Li}$ NMR and ${}^{15}\text{N}$ NMR Spectra. The ${}^6\text{Li}$ NMR spectrum of ${}^6\text{Li}^+\mathbf{1a}^-$ measured at $-111\text{ }^\circ\text{C}$ shows the same trends found in the ${}^{31}\text{P}$ spectrum, i.e., two signals at 4.41 and 3.47 ppm in a 93:7 ratio (Figure 2b). They coalesce at $-90\text{ }^\circ\text{C}$. The most noteworthy point of the spectrum is the splitting of the signal at 4.41 ppm into a doublet of ${}^2J_{\text{PLi}} = 2.6$ Hz, which collapses to a singlet when the spectrum is recorded with phosphorus decoupling (Figure 2c).²⁷ Additionally, ${}^{31}\text{P}$, ${}^6\text{Li}$ -decoupling due to rapid exchange is observed when the temperature is raised to $-96\text{ }^\circ\text{C}$. From this coupling it can be concluded that ${}^6\text{Li}^+\mathbf{1a}^-$ is present mainly as a monomer in THF solution. Any other combination of head-to-tail or head-to-head oligomers would afford a higher splitting of the lithium signal. Cryoscopic measurements in benzene also agree with the existence of a monomer of ${}^6\text{Li}^+\mathbf{1a}^-$ in solution ($n = 0.97 \pm 0.08$). The observation of ${}^2J_{\text{PLi}}$ -coupling is preceded in HMPA-lithium cation complexes, and it has been applied in the characterization

(26) Imhoff, P.; van Asselt, R.; Elsevier, C. J.; Vrieze, K.; Goubitz, K.; van Malssen, K. F.; Stam, C. H. *Phosphorus Sulfur* 1990, 47, 401.

(27) The corresponding ${}^{31}\text{P}$, ${}^7\text{Li}$ -coupling of 6.9 Hz is clearly observed in the ${}^7\text{Li}$ -NMR (155.45 MHz) spectrum of ${}^7\text{Li}^+\mathbf{1a}^-$.

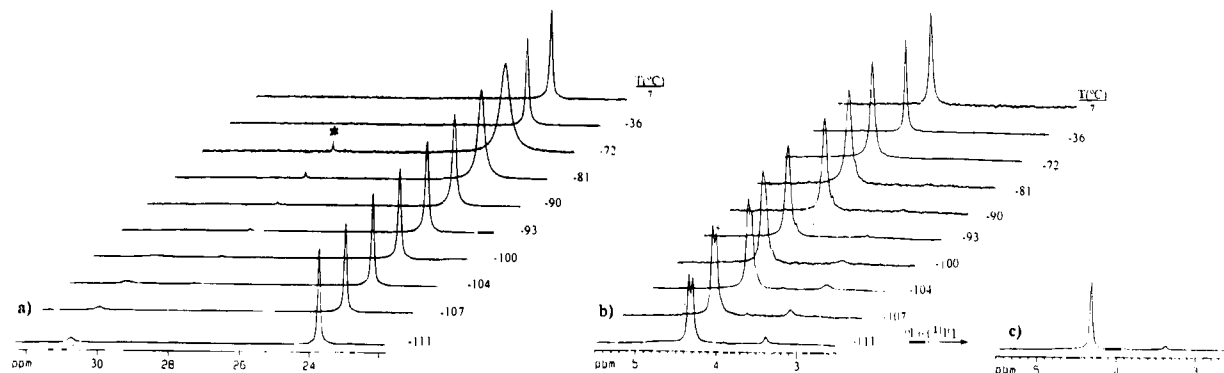


Figure 2. NMR spectra of a solution 0.2 M of $\text{Li}^+\mathbf{1a}^-$ in $\text{THF-}d_8$ at different temperatures: (a) ^{31}P (161.98 MHz) (the signal marked with an asterisk belongs to an impurity; 9% of $\mathbf{1a}$ is observed at 2.04 ppm and is not shown); (b) ^6Li (58.88 MHz); and (c) $^6\text{Li}\{^{31}\text{P}\}$ measured at -111°C .

of lithium ion pair structures in solution.²⁸ Its use as an *internal marker* may provide direct evidence of the aggregation state of the lithiated species.^{11b}

Recording the natural abundance ^{15}N NMR spectrum of $^6\text{Li}^+\mathbf{1a}^-$ is not an easy task because of the low receptivity of the ^{15}N nucleus and the absence of protons suitable for polarization transfer processes.²⁹ However, polarization transfer is not restricted to protons. Any sensitive nucleus can act as a source provided it shares a J -coupling with the target nucleus. For $^6\text{Li}^+\mathbf{1a}^-$, the ^{31}P is the nucleus of choice because of its high sensitivity and the magnitude of the P,N-couplings in phosphazenes.³⁰ ^{15}N Detection using polarization transfer from ^{31}P based on INEPT and DEPT pulse schemes has been recently reported.³¹ The $^{15}\text{N},^{31}\text{P}$ INEPT spectrum of $^6\text{Li}^+\mathbf{1a}^-$ acquired with simultaneous proton decoupling during the whole experiment shows an antiphase doublet at -274.56 ppm of $^1J_{\text{PN}} = 26.8$ Hz. Therefore, lithiation of $\mathbf{1a}$ produces a downfield shift of the nitrogen of 24.6 ppm as well as a decrease of 9.8 Hz in $^1J_{\text{PN}}$ (Table 2).³² The average signal half-width of 15 Hz prevents the observation of a N,Li-coupling.³³

The problem of line broadening in the ^{13}C and ^{15}N NMR spectra can be tackled in another way. If we consider that it is not the result of a still rapid interaggregates dynamic exchange,

(28) (a) Barr, D.; Clegg, W.; Mulvey, R. E.; Snaith, R. *J. Chem. Soc., Chem. Commun.* **1984**, 79. (b) Barr, D.; Doyle, M. J.; Mulvey, R. E.; Raithby, P. R.; Berd, D.; Snaith, R.; Wright, D. S. *J. Chem. Soc., Chem. Commun.* **1989**, 318. (c) Reich, H. J.; Green, D. P.; Phillips, N. H. *J. Am. Chem. Soc.* **1989**, *111*, 3444. (d) Reich, H. J.; Green, D. P. *J. Am. Chem. Soc.* **1989**, *111*, 8729. (e) Romesburg, F. E.; Gilchrist, J. H.; Harrison, A. T.; Fuller, D. J.; Collum, D. B. *J. Am. Chem. Soc.* **1991**, *113*, 5751. (f) Jackman, L. M.; Chen, X. *J. Am. Chem. Soc.* **1992**, *114*, 403. (g) Reich, H. J.; Borst, J. P.; Dykstra, R. R. Green, D. P. *J. Am. Chem. Soc.* **1993**, *115*, 8728 and references therein.

(29) (a) Philipsborn, W. v.; Müller, R. *Angew. Chem., Int. Ed. Engl.* **1986**, *25*, 368. (b) Morris, G. A. *J. Am. Chem. Soc.* **1980**, *102*, 428. Polarization transfer from protons to ^{15}N should be based on the $^3J_{\text{NH}}$ -coupling between the nitrogen and the ortho protons of the phenyl ring bonded to it as well as the protons of the methylene group, which is usually very small. Therefore, significant losses of magnetization are expected due to relaxation during the long delays needed for the evolution of the long-range N,H-coupling.

(30) Witanowski, M.; Stefaniak, L.; Webb, G. A. *Annu. Rep. NMR Spectrosc.* **1986**, *18*, 1.

(31) (a) Price, S. J. B.; DiMartino, M. J.; Hill, D. T.; Kuroda, R.; Mazid, M. A.; Sadler, P. J. *Inorg. Chem.* **1985**, *24*, 3425. (b) Gudat, D. *Magn. Reson. Chem.* **1993**, *31*, 925. (c) Gudat, D.; Link, M.; Schröder, G. *Magn. Reson. Chem.* **1995**, *33*, 59. Gudat, D. *J. Magn. Reson. A* **1995**, *112*, 246.

(32) The ^{15}N chemical shift and $^1J_{\text{PN}}$ of $\mathbf{1a}$ in $\text{THF-}d_8$ are -301.9 ppm and 36.6 Hz, respectively.

(33) The range of $^1J_{\text{N}^6\text{Li}}$ is found between 3 and 10 Hz and is not very sensitive to changes in the aggregation state.^{33a-d} Leading references: (a) DePue, J. S.; Collum, D. B. *J. Am. Chem. Soc.* **1988**, *110*, 5518. (b) Romesburg, F. E.; Gilchrist, J. H.; Harrison, A. T.; Fuller, D. J.; Collum, D. B. *J. Am. Chem. Soc.* **1991**, *113*, 5751. (c) Sakuma, K.; Gilchrist, J. H.; Romesburg, F. E.; Cajthaml, C. E.; Collum, D. B. *Tetrahedron Lett.* **1993**, *34*, 5213. (d) Romesburg, F. E.; Collum, D. B. *J. Am. Chem. Soc.* **1994**, *116*, 9198.

as the lithium doublet suggests, but a problem derived from the low temperatures required,³⁴ then the $^6\text{Li},^{13}\text{C}$ - and $^6\text{Li},^{15}\text{N}$ -coupling could be unraveled through 2D NMR spectroscopy.³⁵ In a first approach, we tried to establish the corresponding scalar connectivity through 2D $^6\text{Li},^{13}\text{C}$ ^{36,36} and $^6\text{Li},^{15}\text{N}$ experiments.³⁷ In both cases, the indirect detection HMQC pulse scheme with lithium-6 observation was used, modified to perform WALTZ16 decoupling of the protons during the whole experiment.³⁸ However, no cross peaks could be detected for any of the trials. This suggests that $^1J_{\text{LiX}}$ -couplings ($\text{X} = ^{13}\text{C}, ^{15}\text{N}$) should be very small; therefore, signal loss could take place during the long delays needed to allow for $^1J_{\text{LiX}}$ evolution.^{15b, 33}

Next, we carried out 2D $^{31}\text{P},^{13}\text{C}$ ³⁹ and $^{31}\text{P},^{15}\text{N}$ heteronuclear⁴⁰ correlations using the same pulse sequence mentioned above. In these experiments, the ^6Li acts as a passive coupling; therefore, the $^6\text{Li},\text{X}$ -coupling ($\text{X} = ^{13}\text{C}$ or ^{15}N) would modulate the double quantum coherences evolving during t_1 as well as the phosphorus magnetization being detected.⁴¹ Therefore, tilted cross peaks should be expected, whose slopes would also reveal the relative sign of the passive J -couplings involved.⁴² The bandwidth in the F1 and F2 dimensions can be very short, allowing high-resolution spectra to be obtained. Only signals for the major component are detected. However, the tilt

(34) Line broadening due to fast scalar relaxation of the second kind should be ineffective based on the slow relaxation rate of ^6Li . Wehrli, F. W. *Org. Magn. Reson.* **1978**, *11*, 106.

(35) (a) Günther, H.; Moskau, D.; Dujardin, R.; Maercker, A. *Tetrahedron Lett.* **1986**, *27*, 2251. (b) Bauer, W.; Feigel, M.; Müller, G.; Schleyer, P. v. R. *J. Am. Chem. Soc.* **1988**, *110*, 6033.

(36) (a) Fraenkel, G.; Henrichs, M.; Hewitt, J. M.; Su, B. M.; Geckle, M. J. *J. Am. Chem. Soc.* **1980**, *102*, 3345. (b) Moskau, D.; Brauers, F.; Günther, H.; Maercker, A. *J. Am. Chem. Soc.* **1987**, *109*, 5532.

(37) (a) Gilchrist, J. H.; Collum, D. B. *J. Am. Chem. Soc.* **1992**, *114*, 794. (b) Gilchrist, J. H.; Harrison, A. T.; Fuller, J.; Collum, D. B. *Magn. Reson. Chem.* **1992**, *30*, 855.

(38) Phosphorus detection has been widely applied to the NMR characterization of low γ nuclei. See, for example: Benn, R.; Jousen, E.; Lehmkühl, H.; López-Ortiz, F.; Rufinska, A. *J. Am. Chem. Soc.* **1989**, *111*, 8754 and references therein.

(39) (a) Sims, L. D.; Soltero, L. R.; Martin, G. E. *Magn. Reson. Chem.* **1984**, *27*, 599. (b) Bast, P.; Berger, S.; Günther, H. *Magn. Reson. Chem.* **1992**, *30*, 587. (c) Beckmann, H.; Grossmann, G.; Ohms, G. *Magn. Reson. Chem.* **1992**, *30*, 860.

(40) López-Ortiz, F.; Peláez-Arango, E. Manuscript in preparation.

(41) The observable magnetization given by the product operators formalism^{41a,b} would include a factor $\cos(\pi J_{\text{XLi}}t_1)$ for the evolution of the $\text{X},^6\text{Li}$ -coupling during t_1 and $\cos(\pi J_{\text{PLi}}t_2)$ for the modulation by $^{31}\text{P},^6\text{Li}$ -coupling during t_2 : (a) Soerensen, O. W.; Eich, G. W.; Levitt, M. H.; Bodenhausen, G.; Ernst, R. R. *Prog. Nucl. Magn. Reson. Spectrosc.* **1983**, *16*, 163. (b) Kessler, H.; Gehrke, M.; Griesinger, C. *Angew. Chem., Int. Ed. Engl.* **1988**, *27*, 490.

(42) (a) Benn, R.; Brenneke, H.; Jousen, E.; Lehmkühl, H.; López-Ortiz, F. *Organometallics* **1990**, *9*, 756. (b) Schmidt, B. B.; Tang, W. C.; Eisenbrand, G.; van der Lieth, C. W.; Hull, W. E. *Magn. Reson. Chem.* **1992**, *30*, 1224. (c) López-Ortiz, F.; Peláez-Arango, E. Palacios, F.; Barluenga, J.; García-Granda, S.; Tejerina, B.; García-Fernández, A. *J. Org. Chem.* **1994**, *59*, 1984.

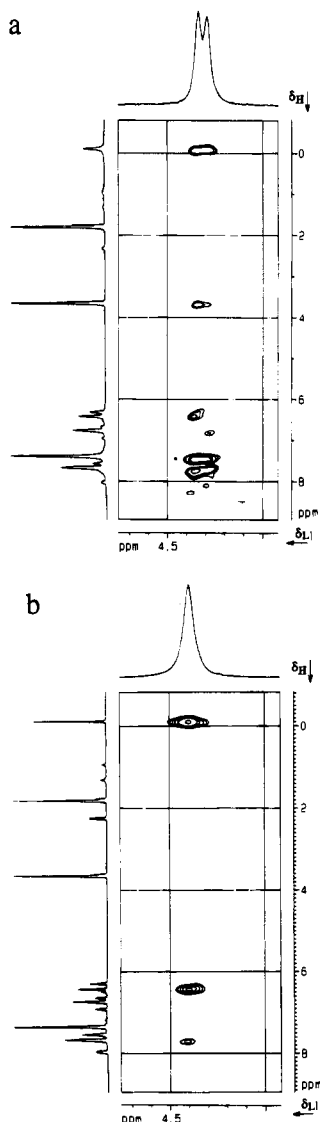


Figure 3. 2D ${}^6\text{Li}, {}^1\text{H}$ HOESY contour plot of $\text{Li}^+\mathbf{1a}^-$ in $\text{THF-}d_8$ (0.2 M) acquired at (a) -111 and (b) -70 $^\circ\text{C}$. The mixing time was set to 2 s in both cases.

observed in the cross peaks of the 2D ${}^{31}\text{P}, {}^{13}\text{C}$ and ${}^{31}\text{P}, {}^{15}\text{N}$ correlation spectra is of the order of the digital resolution, and no definite conclusions can be drawn about the C–Li/N–Li connectivity.

Lithium coordination to the phosphazanyl moiety can be demonstrated on the basis of their spatial proximity. The relationship between spatially close nuclei is currently detected by using NOE experiments. The HOESY variant⁴³ has been extensively employed to establish heteronuclear dipolar ${}^6\text{Li}, {}^1\text{H}$ correlations in the structural analysis of lithiated compounds.⁴⁴ The 2D ${}^6\text{Li}, {}^1\text{H}$ HOESY spectrum of $\text{Li}^+\mathbf{1a}^-$ (Figure 3a) shows strong NOE cross peaks of the ${}^6\text{Li}$ with the protons of the phenyl rings bonded to phosphorus and the methylenic protons of C1, as well as two less intense correlations with H3/H7 (6.45 ppm) and the signal at 3.65 ppm, corresponding to the most deshielded protons of the THF.

The NOEs observed in the HOESY spectrum are consistent with the information derived from the ${}^{31}\text{P}, {}^6\text{Li}$ -coupling constant

and support the similarity between the solid-state and solution-state structure of $\text{Li}^+\mathbf{1a}^-$. But the relative intensity of the cross peaks in the aromatic protons region is noteworthy. Among other factors, the NOE intensity is proportional to $1/r^6$, where r is the distance between the dipolarly relaxing nuclei. Thereby the NOE decays very rapidly as r increases with an upper limit of detection of 5 Å. On these grounds, no NOE correlation should be expected between the Li and the meta protons of the *P*-phenyl rings. However, the HOESY spectrum shows a large cross peak correlating these nuclei. Furthermore, in the solid state, the ortho protons of the *N*-phenyl ring are closer to the lithium atom than those of the *P*-phenyl rings (2.902 vs 3.764 Å). Therefore, the ${}^6\text{Li}$ should afford a larger NOE with H3/H7 than with H9/H13/H15/H19. On the contrary, the opposite is observed. Since the multiplicity of the lithium signal ruled out the formation of head-to-tail oligomers, the NOEs observed can be explained in two ways: (i) assuming conformational differences between the solution-state and solid-state structures so that in solution the lithium would move out of the plane defined by the C1–P1–N1 atoms, thus approaching the *P*-phenyl rings, or (ii) as a transferred NOE from the minor species present in solution to the monomer due to chemical exchange. When the experiment is repeated at -70 $^\circ\text{C}$, the cross peak at 7.45 ppm in F1 disappears and the intensities of the correlations at 6.45 and 7.71 ppm are reversed in relation to those in the spectrum obtained at lower temperature (Figure 3b).

MNDO Calculated Structures of $\mathbf{1a}$ and $\text{Li}^+\mathbf{1a}^-$. Taking into account the solid-state structure of $\text{Li}^+\mathbf{1a}^-$, we wondered what would be the driving force for the four-membered ring formation and how stable it would be. We have used a theoretical approach to answer these questions. The geometry of $\mathbf{1a}$ has also been optimized and will be used as a reference to explain the changes induced by the metalation process leading to $\text{Li}^+\mathbf{1a}^-$.

The predicted minimum energy structure of $\mathbf{1a}$ (see supporting information) corresponds to the *gauche* arrangement along the P1–C1 bond, where the *P*-phenyl rings adopted the propeller-like orientation commonly found in diphenyl- and triphenylphosphoryl groups. The *N*-phenyl ring is almost coplanar with the P=N moiety (cf. P1–N1–C2–C3 torsion angle of 170°) and bisects the C8–P1–C14 bond angle. The P1–C1 bond distance (1.80 Å) lies in the expected range for a formal single bond,²⁶ whereas the P1–N1 bond length (1.64 Å) is found midway of the typical values for formal P–N and P=N bonds.^{23,24}

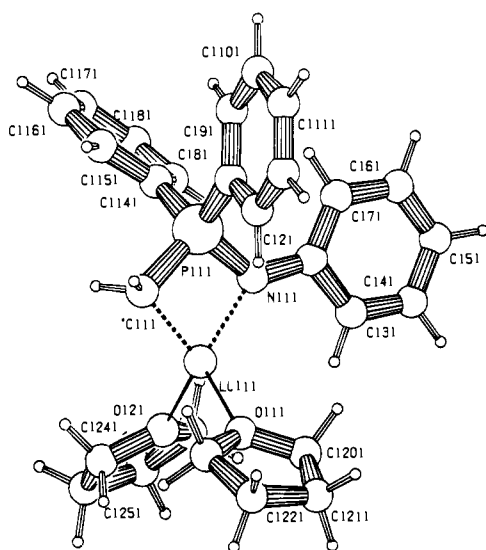
For $\text{Li}^+\mathbf{1a}^-$, the MNDO calculations predict the formation of an almost planar four-membered ring as the most stable configuration (cf. torsion angle C1–P1–N1–Li1 of -0.8°), and the corresponding conformation is also in very good agreement with that found in the solid state (Figure 4, Table 3). In relation to $\mathbf{1a}$, the net effect of the metalation seems to have forced the CH₂ protons to be eclipsed with the *P*-phenyl rings due to the ring formed. C1, P1, and N1 have retained their formal hybridization, but some deviations from the geometry of the four-membered ring formed in the crystal are evident. Thus, the calculated P1–N1 bond distance in $\text{Li}^+\mathbf{1a}^-$ increases only slightly versus that of $\mathbf{1a}$ and is too short compared to that found in the crystal. But larger discrepancies are observed for the P1–C1–Li1 moiety. In comparison with those experimentally obtained, the calculated P1–C1 and C1–Li1 distances are too long and too short, respectively. This may be a consequence of the known overestimation of the C–Li bond strength by the MNDO method.⁴⁵ Even so, the agreement between the calculated and solid-state structures of $\text{Li}^+\mathbf{1a}^-$ can be considered very good.

(43) (a) Rinaldi, P. L. *J. Am. Chem. Soc.* **1983**, *105*, 5167. (b) Yu, C.; Levi, G. C. *J. Am. Chem. Soc.* **1984**, *106*, 6533.

(44) (a) Bauer, W.; Müller, G.; Pi, R.; Schleyer, P. v. R. *Angew. Chem., Int. Ed. Engl.* **1986**, *25*, 1103. (b) Bauer, W.; Winchester, W. R.; Schleyer, P. v. R. *Organometallics* **1987**, *6*, 2371. (c) For an extensive bibliography of 2D ${}^6\text{Li}, {}^1\text{H}$ HOESY, see ref 15d.

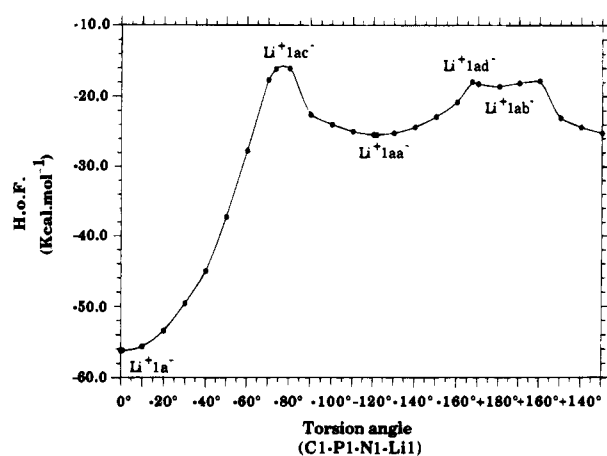
Table 3. Heats of Formation and Selected Geometric Parameters Calculated for the Minima Located by MNDO in the Evolution of the C1–P1–N1–Li1 Torsion Angle of $\text{Li}^+1\mathbf{a}^-$

ΔH° (kcal mol $^{-1}$)	bond lengths (Å)	bond angles (deg)	torsion angles (deg)
$\text{Li}^+1\mathbf{a}^-$, -56.2	P1–N1 = 1.66 P1–C1 = 1.84 C1–Li = 2.00 N1–Li = 2.19	C1–P1–N1 = 99.3 Li–N1–P1 = 90.2 C1–Li–N1 = 79.0 Li–C1–P1 = 91.5 C2–N1–P1 = 127.9	N1–P1–C1–Li = 0.9 P1–N1–C2–C3 = 175.2 C1–P1–N1–C2 = -170.7 H1–C1–P1–N1 = 126.2 C8–P1–C1–H1 = 8.1
$\text{Li}^+1\mathbf{aa}^-$, -25.4	P1–N1 = 1.66 P1–C1 = 1.64 C9–Li = 2.40 N1–Li = 2.07	C1–P1–N1 = 116.1 P1–N1–C2 = 125.0 C9–Li–N1 = 87.0 Li–N1–P1 = 113.0 Li–C9–C8 = 84.5	C1–P1–N1–Li = -121.6 C1–P1–N1–C2 = 45.1 P1–N1–Li–C9 = -24.3 H1–C1–P1–N1 = -151.7 C8–P1–C1–H1 = 97.3
$\text{Li}^+1\mathbf{ab}^-$, -18.6	P1–N1 = 1.66 P1–C1 = 1.65 C7–Li = 2.36 N1–Li = 2.07 C2–Li = 2.45	C1–P1–N1 = 116.1 C2–N1–P1 = 123.5 Li–C2–N1 = 57.7 Li–C2–C7 = 68.9 C7–Li–N1 = 65.1 Li1–C7–C2 = 74.0 C2–N1–Li1 = 86.2	C1–P1–N1–Li = 180.0 C1–P1–N1–C2 = 30.6 P1–N1–Li–C7 = -34.8 P1–N1–C2–C7 = -158.1 N1–P1–C1–H1 = -149.4

**Figure 4.** MNDO calculated structure of minimum energy of $\text{Li}^+1\mathbf{a}^-$. Hydrogen atoms are omitted for clarity.

In order to estimate the stability of the four-membered ring of $\text{Li}^+1\mathbf{a}^-$, we have studied the evolution from the four-membered ring to acyclic structures using the torsion angle C1–P1–N1–Li1 as reaction coordinate. A plot of the heat of formation versus the torsion angle $\phi = \text{C1–P1–N1–Li1}$ is depicted in Figure 5, and the calculated heats of formation are given in Tables 3 and 4. Interestingly, two new minima as well as two maxima were found in the potential energy surface. The minima would be abbreviated as $\text{Li}^+1\mathbf{aa}^-$ and $\text{Li}^+1\mathbf{ab}^-$, and the maxima would be $\text{Li}^+1\mathbf{ac}^-$ and $\text{Li}^+1\mathbf{ad}^-$. Once these points were located their geometries were fully optimized. The frequency analysis indicates that $\text{Li}^+1\mathbf{aa}^-$ is a local minimum and that $\text{Li}^+1\mathbf{ac}^-$ and $\text{Li}^+1\mathbf{ad}^-$ correspond to transition states in the PES. Instead, the optimization of $\text{Li}^+1\mathbf{ab}^-$ afforded $\text{Li}^+1\mathbf{aa}^-$ as final geometry (Figure 6).

In $\text{Li}^+1\mathbf{aa}^-$, the torsion angle C1–P1–N1–Li1 is -121.6° and the C1–Li1 bond no longer exists, so the lithium atom completes the coordination sphere by bonding to the ortho carbon of one of the *P*-phenyl rings (Li1–C9 distance of 2.39 Å). Accordingly, the C1 shows an sp^2 hybridization, and consequently the P1–C1 bond length is reduced to 1.64 Å. The

**Figure 5.** MNDO calculated heats of formation of the structures obtained by increasing the torsion angle C1–P1–N1–Li1 of $\text{Li}^+1\mathbf{a}^-$.

P1–N1 distance remains unchanged relative to $\text{Li}^+1\mathbf{a}^-$. The CH_2 lies rotated out of the C1–P1–N1 plane (torsion angle N1–P1–C1–H2 of 36.7°), whereas the *N*-phenyl ring has apparently rotated slightly out of the plane defined by the phosphazenyli moiety. In fact, this ring has performed almost a 180° rotation around the N1–C2 bond (cf. torsion angle P1–N1–C2–C3 of 175.1° for $\text{Li}^+1\mathbf{a}^-$ and 13.7° for $\text{Li}^+1\mathbf{aa}^-$).

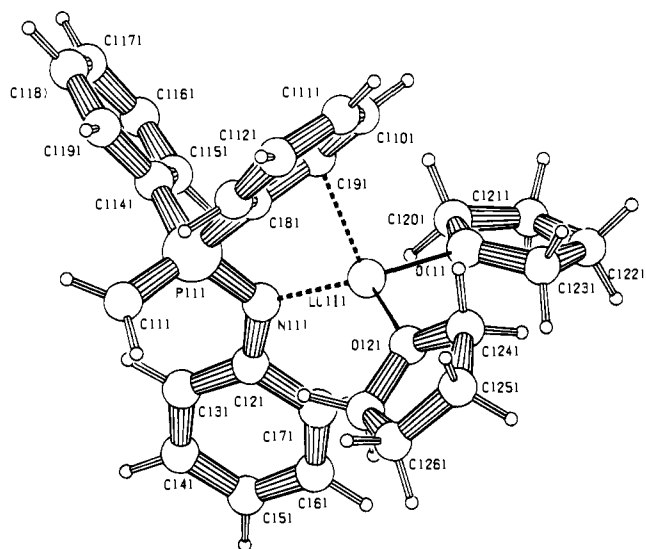
At $\phi = 180^\circ$, an apparent minimum is observed, $\text{Li}^+1\mathbf{ab}^-$. Now, the lithium shows a η^3 coordination to N1–C2–C7, thus forming a new four-membered ring. However, when the full geometry optimization is carried out, no convergence is observed, so the structure is considered an artifact of the computational method. On the other hand, the harmonic vibrational frequency analysis of $\text{Li}^+1\mathbf{ac}^-$ and $\text{Li}^+1\mathbf{ad}^-$ indicates that they can be considered as the transition states interconverting at the minima located. Their heats of formation are similar ($\Delta H^\circ_{\text{Li}^+1\mathbf{ac}^-} - \Delta H^\circ_{\text{Li}^+1\mathbf{ad}^-} = 1.9 \text{ kcal}\cdot\text{mol}^{-1}$), but their structures are very different. In $\text{Li}^+1\mathbf{ac}^-$ ($\phi = -73.5^\circ$), the lithium cation is close to C13, a carbon atom belonging to one of the *P*-phenyl rings. Instead, for $\text{Li}^+1\mathbf{ad}^-$ ($\phi = 167.0^\circ$), the lithium is found η^3 coordinated to the N1–C2–C7 fragment of the *N*-phenyl group. Selected geometric parameters for these structures are given in Table 4.

In the evolution from $\text{Li}^+1\mathbf{a}^-$ to $\text{Li}^+1\mathbf{aa}^-$, the C–Li bond is broken, and the energy difference between these species of $30.8 \text{ kcal}\cdot\text{mol}^{-1}$ can be taken as an indication of the dissociation energy of the C1–Li1 bond. This value correlates well with

(45) (a) Würthwein, E. U.; Sen, K. D.; Pople, J. A.; Schleyer, P. v. R. *Inorg. Chem.* **1983**, *22*, 496. (b) Kaufmann, E.; Raghavachari, K.; Reed, A. E.; Schleyer, P. v. R. *Organometallics* **1988**, *7*, 1597.

Table 4. Heats of Formation and Selected Geometric Parameters Calculated for the Transition States Located by MNDO in the Evolution of the C1–P1–N1–Li1 Torsion Angle of Li⁺1a⁻

ΔH° (kcal mol ⁻¹)	bond lengths (Å)	bond angles (deg)	torsion angles (deg)
Li ⁺ 1ac ⁻ , -16.0	P1–N1 = 1.67 P1–C1 = 1.65 C13–Li = 2.44 N1–Li = 2.12	C1–P1–N1 = 109.0 C13–Li–N1 = 96.8 Li–N1–C2 = 131.0 Li–N1–P1 = 97.6 C2–N1–P1 = 127.3	C1–P1–N1–C2 = 127.5 C1–P1–N1–Li = -73.5 Li–N1–C2–C3 = 61.2 P1–C8–C13–Li = 64.1 H1–C1–P1–N1 = 126.2 C8–P1–N1–H1 = 98.7
Li ⁺ 1ad ⁻ , -17.9	P1–N1 = 1.66 P1–C1 = 1.65 C7–Li = 2.36 N1–Li = 2.06 C2–Li = 2.41	C1–P1–N1 = 117.7 C2–N1–P1 = 123.4 Li–C2–N1 = 58.8 Li–C2–C7 = 70.5 C7–Li–N1 = 65.3 Li1–C7–C2 = 74.0 C2–N1–Li1 = 86.2	C1–P1–N1–Li = 167.0 C1–P1–N1–C2 = 30.6 P1–N1–Li–C7 = -34.8 P1–N1–C2–C7 = -158.1 N1–P1–C1–H1 = -149.4 C8–P1–C1–H1 = 111.8 Li1–N1–C2–C7 = 43.8

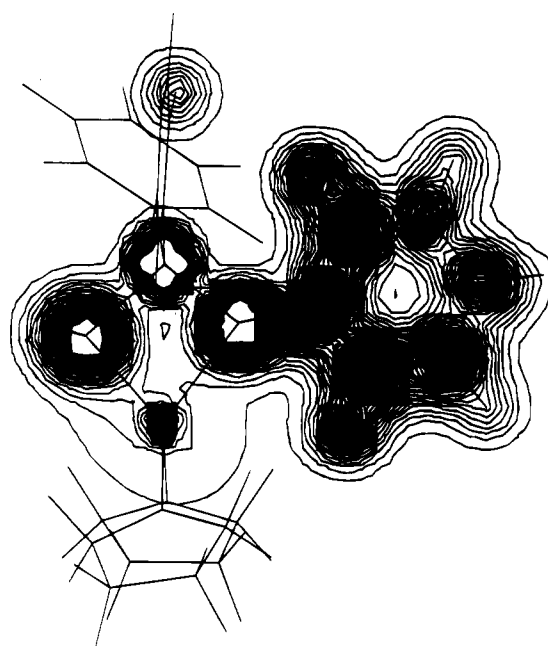
**Figure 6.** MNDO optimized structure of the lowest energy saddle point (Li⁺1aa⁻) located on the PES in the rotation of the torsion angle C1–P1–N1–Li1 of Li⁺1a⁻. Hydrogen atoms are omitted for clarity.

the calculated dissociation energy for methyllithium.⁴⁶ The MNDO calculations performed on ⁶Li⁺1a⁻ also serve to shed some light on the factors governing the formation of the four-membered ring. We have tackled the problem in two ways: (i) by considering the electronic density of the C–Li and N–Li bonds and (ii) by calculating the partial charges of the atoms taking part in the ring. A plot of the total electronic density in the C1–Li1–N1 plane is depicted in Figure 7. According to this, there is no electronic density connecting the P and Li atoms, and it is very low between the C–Li and N–Li bonds. This would imply that the lithium is held close to the carbon and nitrogen atoms of the phosphazene moiety due to internal Coulombic stabilization, thus indicating a very low covalent bonding contribution to the C–Li and N–Li bonds. Curiously, the Mulliken analysis afforded relative low partial charges for C1, N1, and Li1 (supporting information), but this is known to be an artifact of the method, which underestimates the ionic contribution to the C–Li bond in organolithium compounds.

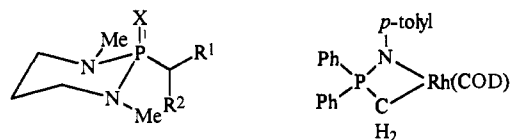
Discussion

When ⁶Li⁺1a⁻ is compared to some related phosphorus-stabilized anions of known structure,¹¹ e.g., **2** and **3**, three main

(46) (a) Imhoff, P.; Elsevier, C. J. *J. Organomet. Chem.* **1989**, *361*, C61. (b) Elsevier, C. J.; Imhoff, P. *Phosphorus Sulfur* **1990**, *49*, 405. (c) Imhoff, P.; Nefkens, S. C. A.; Elsevier, C. J.; Goubitz, K.; Stam, C. H. *Organometallics* **1991**, *10*, 1421. See also: (d) Imhoff, P.; van Asselt, R.; Elsevier, C. J.; Zoutberg, M. C.; Stam, C. H. *Inorg. Chim. Acta* **1991**, *184*, 73.

**Figure 7.** Plot of the total electron density in the C1–N1–Li1 plane of Li⁺1a⁻ generated by the DENDIF program implemented in GAMESS.²¹ The plot contains 299 contours spaced at 0.01 au. The minimum density plotted is 0, and the maximum is 310. Minimum and maximum contours are drawn at 0 and 2.99 au, respectively.

differences are evident: (i) carbanion ⁶Li⁺1a⁻ is a monomer in solution and in the solid state, (ii) there is C–Li contact, and (iii) the metalated carbon remains sp³ hybridized. In fact,

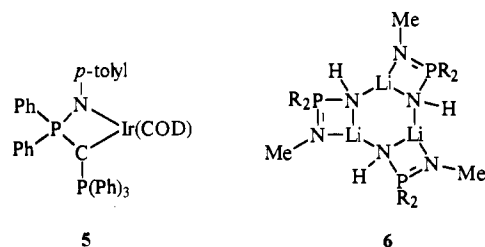


2a: X = O; R¹ = H; R² = C₆H₅

2b: X = O; R¹ = R² = CH₃

3: X = S; R¹ = H; R² = C₆H₅

4



5

6

the structure of ${}^6\text{Li}^+\mathbf{1a}^-$ resembles that of some rhodium⁴⁶ **4** and iridium⁴⁷ **5** complexes of monophosphazenes, where the phosphazanyl moiety behaves as a bidentate ligand. Also similar is the crystal structure of lithiated *P*-diphenyl-*N,N*-bis-(trimethylsilyl)phosphazene,⁴⁸ which exhibits equal P–N and N–Li bond lengths in the four-membered ring formed. Earlier cryoscopic measurements in benzene on the structurally related lithium salt of *N*-methyl-*P*-di-*tert*-butylphosphazene showed that it formed trimers in solution, for which the structure **6** was tentatively proposed,⁴⁹ but no further experimental evidence was given.

It has been suggested that intramolecular metal coordination to nitrogen and carbon represents a particularly stable configuration for metalated phosphazenes due to an increase in the polarization within the ring.^{46c} The mainly ionic nature of the C–Li bond in organolithium compounds is now widely accepted,⁵⁰ but the existence of C,Li-couplings is attributed to a small covalent contribution. Furthermore, these couplings depend not on the carbon hybridization but on the aggregation, and it has been empirically^{44b} found that they follow the equation ${}^1J_{\text{C-Li}} = (17 \pm 2)n$, where n is the number of lithium atoms directly bonded to a carbon atom. Therefore, a large C,Li-coupling should be expected for ${}^6\text{Li}^+\mathbf{1a}$ under slow interaggregate exchange conditions. The validity of this condition is deduced from the observation of a ${}^2J_{\text{P-Li}}$ -coupling. However, no C,Li-coupling could be measured. Significant deviations from the above equation have been found for monomeric organolithium compounds, which showed C,Li-coupling lower than expected as the ionic character of the C–Li bond increases. Thus, no C,Li-coupling has been detected for monomeric benzyl lithium in THF at very low temperatures.⁵¹ Lower ${}^1J_{\text{C-Li}}$ values than expected have also been found in α -lithium sulfur compounds.⁵² From the 2D ${}^{31}\text{P}$, ${}^{13}\text{C}$ spectrum of ${}^6\text{Li}^+\mathbf{1a}^-$, an upper limit of 1 Hz can be estimated for ${}^1J_{\text{C-Li}}$. This small value would be consistent with a very high ionic bonding contribution to the C–Li bond, in agreement with the MNDO calculations, and would reinforce the proposal of electrostatic forces being responsible for the formation of the four-membered ring in ${}^6\text{Li}^+\mathbf{1a}$. Similarly, a high ionic character can be assigned to the N–Li bond from the estimated value of ${}^1J_{\text{N-Li}} = 1$ Hz from the 2D ${}^{31}\text{P}$, ${}^{15}\text{N}$ spectrum.

In this ring, the P–Li distance lies within the limits of a real bond, implying pentacoordination for lithium. Although lithium coordinations other than 4 are known,^{13c,53} we wanted to check whether there is a real P–Li bonding interaction in the anion ${}^6\text{Li}^+\mathbf{1a}^-$ or if the observed distance is a consequence of the geometry of the ring. The experimental parameter relating these nuclei would be the ${}^2J_{\text{P-Li}}$ -coupling, which is of the order of that found in solvent-separated ion pairs complexed with HMPA²⁸ (7.7 Hz; ${}^7\text{Li}$ isotope). For contact ions, ${}^2J_{\text{P-Li}}$ increases gradually

(47) Imhoff, P.; van Asselt, R.; Ernsting, J. M.; Vrieze, K.; Elsevier, C. J.; Smeets, W. J. J.; Spek, A. L.; Kentgens, A. P. M. *Organometallics* **1993**, *12*, 1523.

(48) (a) Recknagel, A.; Steiner, A.; Noltemeyer, M.; Brooker, S.; Stalke, D.; Edelmann, F. *J. Organomet. Chem.* **1991**, *414*, 327. (b) Steiner, A.; Stalke, D. *Inorg. Chem.* **1993**, *32*, 1977. (c) Also related is the structure of the lithium tris(imino)metaphosphate, Niecke, E.; Frost, M.; Nieger, M.; Gönna, V. v. d.; Ruban, A.; Schoeller, W. W. *Angew. Chem., Int. Ed. Engl.* **1994**, *33*, 2111.

(49) Sherer, O. J.; Schieder, G. *J. Organomet. Chem.* **1969**, *19*, 315.

(50) Lambert, C.; Schleyer, P. v. R. *Angew. Chem., Int. Ed. Engl.* **1994**, *33*, 1129.

(51) Seebach, D.; Hässig, R.; Gabriel, J. *Helv. Chim. Acta* **1983**, *66*, 308.

(52) Seebach, D.; Hässig, R.; Gabriel, J. *Helv. Chim. Acta* **1984**, *67*, 1083.

(53) For some recent examples, see: (a) Sekiguchi, A.; Sugai, Y.; Ebata, K.; Kabuto, C.; Sakurai, H. *J. Am. Chem. Soc.* **1993**, *115*, 1144. (b) Lambert, C.; Hampel, F.; Schleyer, P. v. R. *J. Chem. Soc., Chem. Commun.* **1993**, 1773. (c) Li, J. J.; Sharp, P. R. *Inorg. Chem.* **1994**, *33*, 183.

(9.3–11.1 Hz) with the decreasing number of HMPA molecules coordinated to the lithium. Since the presence of solvent-separated ions has been previously excluded, the small ${}^2J_{\text{P-Li}}$ in ${}^6\text{Li}^+\mathbf{1a}^-$ (6.9 Hz for the ${}^7\text{Li}$ isotope) could be explained in two ways: (i) as the algebraic sum of ${}^1J_{\text{P-Li}}$ and ${}^2J_{\text{P-Li}}$ of opposite sign or (ii) as a consequence of the structural factors affecting ${}^2J_{\text{P-Li}}$, i.e., dependence on the valence angles and/or atomic densities at the coupled nuclei⁵⁴ in the four-membered ring. In the first case, a P–Li bonding interaction is implied, whereas in the second it is not. However, according to the rule that for a pair of nuclei ${}^1J \gg {}^2J$, it does not seem reasonable that the positive one-bond coupling would be compensated by the negative ${}^2J_{\text{P-Li}}$, even though two ${}^2J_{\text{P-Li}}$ -coupling paths are possible for ${}^6\text{Li}^+\mathbf{1a}^-$. Another argument against the existence of P–Li interactions is obtained from the electronic density plot shown above. Figure 7 shows that the nitrogen and carbon atoms share some electronic density with the lithium atom, but this is not the case for the phosphorus and lithium atoms. Therefore, a P–Li bonding interaction can be excluded.

Chemical shifts variations of ${}^6\text{Li}^+\mathbf{1a}^-$ vs **1a** can be reasonably explained in terms of charge density modifications. Thus, the calculated Mulliken charges predicted an increase in the negative charge of C1 when metalated, and consequently, C1 and H1 are strongly shifted to higher fields. Also C3, C5, and their attached protons appear slightly shielded in ${}^6\text{Li}^+\mathbf{1a}^-$, which can be attributed to the resonance delocalization of the negative charge into the *N*-phenyl ring.⁵⁵ N1 shows the opposite trend, i.e., a decrease of the negative charge and therefore a deshielding of 24.6 ppm relative to **1a**. However, the positive charges obtained for P1 and Li1 are too small to account for their chemical shifts. It must be remembered that chemical shifts are the result of several contributions and that the Mulliken analysis tends to overestimate the covalent contribution to the C–Li bond. For example, large downfield ${}^{31}\text{P}$ shifts have been observed upon deprotonation of phosphonamides,^{11a,b} but the ${}^{31}\text{P}$ signal of lithiated thiophosphonamides was shifted to higher fields.^{11c}

The changes in ${}^1J_{\text{P-X}}$ ($X = {}^{13}\text{C}$, ${}^{15}\text{N}$) by metalation of **1a** are also noteworthy, especially the increase of ${}^1J_{\text{P-C1}}$ and the decrease of ${}^1J_{\text{P-C18/14}}$ and ${}^1J_{\text{P-N1}}$. Conventional wisdom tells us that these coupling constants are dominated by the Fermi contact term. In the McConnell model of spin–spin coupling, this term is proportional to $(\text{Psp}_X)^2(\Delta E)^{-1}$, where $(\text{Psp}_X)^2$ represents the bond order and ΔE is the average ground-state to triplet-state excitation energy. Thus, a larger ${}^1J_{\text{P-C1}}$ would correspond to a shorter P1–C1 in ${}^6\text{Li}^+\mathbf{1a}^-$ vs **1a**, and consequently, the increase in the P1–N1 bond length of ${}^6\text{Li}^+\mathbf{1a}^-$ would afford a smaller ${}^1J_{\text{P-N1}}$ -coupling, as is observed. However, the P1–C8/14 bond length is of the same order as that found in related nonmetalated monophosphazenes.²⁴ Assuming a dependence of ${}^1J_{\text{C-H}}$ and ${}^1J_{\text{P-C}}$ on similar factors,^{54b} the small value of ${}^1J_{\text{P-C8/14}}$ in ${}^6\text{Li}^+\mathbf{1a}^-$ could then be attributed to changes in the geometry of the phosphorus atom imposed by the four-membered ring and to rehybridization induced by changes in the charge distribution of metalated **1a**. Recent maximum bond order hybrid orbital (MBOHO) calculations of C–H coupling constants showed that the best fit between experimental and theoretical data was obtained when

(54) (a) Jameson, C. J. In *Phosphorus-31 NMR Spectroscopy in Stereochemical Analysis. Organic Compounds and Metal Complexes*; Verkade, J. G., Quin, L. D., Eds.; VCH: New York, 1987; Chapter 6, p 205. (b) Bentrude, W. G.; Setzer, W. N. In ref 54a, Chapter 11, p. 365.

(55) (a) Albright, T. A.; Freeman, W. J.; Schweizer, E. E. *J. Org. Chem.* **1976**, *41*, 2716. (b) Pomerantz, M.; Ziemnicka, B. T.; Merchant, Z. M.; Chou, W. N.; Perkins, W. B.; Bittner, S. *J. Org. Chem.* **1985**, *50*, 1757. (c) Pomerantz, M.; Marynick, D. S.; Rajeshwar, K.; Chou, W. N.; Throckmorton, L.; Tsai, E. W.; Chen, P. C. Y.; Cain, T. J. *J. Org. Chem.* **1986**, *51*, 1223. (d) Chou, W. N.; Pomerantz, M. *J. Org. Chem.* **1991**, *56*, 2762.

the net charges of the C and H atoms were taken into account.⁵⁶ Another possible contribution to the decrease of $^1J_{PC8/14}$ would be a $p\pi-\sigma^*$ interaction of the electronic density on nitrogen with a σ^* antibonding orbital of the P-C8/P-C14 bond, as has been suggested to occur in *N*-aryltriphenylphosphazenes.^{55c,57} The participation of σ^* orbitals would lengthen the P-C8/P-C14 bonds, and their scalar coupling would decrease. In fact, the MNDO optimized structures for **1a** and $^6Li^+1a^-$ predicted an average increase of the P-C8/P-C14 bond lengths for the lithiated compound.

Another interesting point derived from the metalation of **1a** is the very small value measured for $^2J_{PH} = 0.8$ Hz at room temperature for the methylenic protons. Large changes in $^2J_{PH}$ of α -metalated phosphonates have been interpreted in terms of carbon rehybridization^{9b,c} because of the sign dependency of $^2J_{PH}$ upon the geometry of the carbon: $^2J_{PH}$ is negative for sp^3 hybridized carbons,⁵⁸ while it is positive when the carbon is sp^2 hybridized.⁵⁹ However, C1 in $^6Li^+1a^-$ remains pyramidal, as shown by the crystal structure and the value of $^1J_{CH} = 132.9$ Hz. Moreover, $^2J_{PH}$ is negative in both neutral and lithiated **1a**.⁶⁰

It is known for phosphine oxides and sulfides that $^2J_{PH}$ shows a dependence on the dihedral angle α formed between the P=X (X = O, S) double bond and the C-H bond.^{54b} Larger negative values ranging from -13 to -20 Hz have been found for $\alpha \cong 0-60^\circ$. For $\alpha \cong 180^\circ$, they lie between 0 and -6 Hz. Assuming a similar behavior for phosphine oxides and monophosphazenes, and based on the torsion angles H1-C1-P1-N1 of 78.4° and H2-C1-P1-N1 of 148.4° , a $^2J_{PH}$ much larger than that actually observed should be expected. The discrepancy between the expected and experimentally measured values of $^2J_{PH}$ may be attributed to the high ionic character of the C1-Li1 bond in a way resembling the effect of lone pair electrons on $^2J_{PH}$ in trivalent phosphorus compounds.^{54b}

In relation with the minor component found in solution, the information available is limited to the 6Li and ^{31}P chemical shifts measured at -111 °C. Its low concentration and the large width of the signals precluded the observation of any structural correlation. Moreover, any comparison between this compound and the calculated structure for $^6Li^+1aa^-$ seems unreasonable because the energy differences calculated for the local minima in the potential energy surface are too high to account for the 93:7 relation experimentally determined. In fact, the results of the MNDO conformational analysis should be interpreted as a way to estimate the strength of the C-Li bond of $^6Li^+1a^-$. We have forced the four-membered ring to break by increasing the C1-P1-N1-Li1 angle, and the system evolved trying to restore the tetracoordination of the lithium cation by approaching the nearest phenyl ring because there were no other ligands available.

(56) Zhan, C. G.; Hu, Z. M. *Magn. Reson. Chem.* **1994**, *32*, 465.

(57) Gray, G. A.; Albright, T. A. *J. Am. Chem. Soc.* **1977**, *99*, 3243.

(58) McFarlane, W. *Proc. R. Soc. London, Ser. A* **1968**, *306*, 185.

(59) (a) Lancaster, J. E. *Spectrochim. Acta, Part A* **1967**, *23*, 1449. (b) Lequan, R.; Simonnin, M. P. *Bull. Soc. Chim. Fr.* **1973**, 2365. (c) Simonnin, P.; Charrier, C. *Org. Magn. Reson.* **1969**, *1*, 27.

(60) Sign assignments were made from the 2D $^1H,^{13}C$ HMQC correlation spectrum of a sample containing a mixture of **1a** and $^6Li^+1a^-$ in a ratio 1:3. See supporting information.

Summary

The X-ray analysis of $^6Li^+1a^-$ shows that it crystallizes as a monomer where the metal is chelated by the α -lithiated phosphazenylium moiety. This implies that the lithium atom is coordinated to both the carbon and nitrogen atoms and forms a four-membered ring. The metal completes the coordination sphere by bonding to two THF molecules. In solution, two different compounds are detected by multinuclear NMR (1H , 6Li , ^{13}C , ^{15}N , and ^{31}P) spectroscopy. Experimental evidence based on $^2J_{PLi}$ couplings and HOESY spectra indicates that in solution, the major component (93%) retains a structure similar to that found in the solid state. On the other hand, the ^{15}N chemical shift and the $^{31}P,^{15}N$ -coupling constant of $^6Li^+1a^-$ have been obtained through $^{31}P,^{15}N$ triple resonance experiments.

MNDO calculations also predict a minimum energy for the monomer of $^6Li^+1a^-$. The preference for the four-membered ring formed is assigned to Coulombic stabilization, which implies a mainly ionic character for the C-Li and N-Li bonds. Furthermore, a P-Li bonding interaction is excluded. The dissociation energy calculated for the C-Li bond is of the same order as that obtained for methyllithium, and this may be an interesting point for the future prospects of phosphazenylium anions in asymmetric synthesis.

The design of P-stabilized anions that could be used as effective chiral auxiliaries is based on the existence of high rotational barriers⁶¹ around the P-C bond, and this condition might be fulfilled in compounds of the type of $^6Li^+1a^-$ because of the formation of the four-membered ring. Further work is in progress in order to identify the structure of the minor species found in solution and to assess the utility of these reagents in enantioselective synthesis.

Acknowledgment. This work was supported by the DIGI-CYT (PB93 1005). E.P.-A. thanks the Ministerio de Educación y Ciencia for a predoctoral fellowship.

Supporting Information Available: Listing of tables of bond distances, bond angles, torsion angles, atomic coordinates, and thermal parameters for Li^+1a^- , and plots showing the unit cell, crystal packing, and short intermolecular contacts; plots of the MNDO optimized structures of Li^+1a^- , Li^+1aa^- , Li^+1ab^- , Li^+1ac^- , and Li^+1ad^- , and tables including their full geometric parameters and selected partial charges obtained by the Mulliken analysis for each conformer; and the 1H NMR, ^{13}C NMR, and $^{15}N,^{31}P\{^1H\}$ INEPT spectra measured in THF at room temperature and -111 °C, 2D $^{31}P,^{13}C$ and $^{31}P,^{15}N$ HMQC correlation spectra at -111 °C, and 2D $^1H,^{13}C$ HMQC contour plots of the methylene regions of **1a** and Li^+1a^- (50 pages). This material is contained in many libraries on microfiche, immediately follows this article in the microfilm version of the journal, can be ordered from the ACS, and can be downloaded from the Internet; see any current masthead page for ordering information and Internet access instructions.

JA951068V

(61) Aggarwal, V. K. *Angew. Chem., Int. Ed. Engl.* **1994**, *33*, 175 and references therein.